

SYNTHESIS AND CHARACTERIZATION OF NANOSCALE TRANSITION METAL NITRIDES AND CARBIDES FROM METALORGANIC AND HALOGENATED PRECURSORS

R.Ochoa¹, ²P. Zhou, ²W.T. Lee, ²A. Rao, ⁴S. Bandow, and ^{1,2}P.C. Eklund

¹Center for Applied Energy Research, ²Department of Physics and Astronomy,³

Department of Materials Science and Engineering, University of Kentucky, Lexington KY 40506. ⁴Instrument Center, Institute for Molecular Science, Myodajji Okazaki, 444 Japan.

KEYWORDS: Laser Pyrolysis, molybdenum nitride, molybdenum carbide

INTRODUCTION

High surface area ultrafine particle catalysts offer a large number of advantages compared to conventional catalysts: no diffusion resistance, high accessibility of reactants to the active centers of the catalyst, and a large number of active sites per particle. In coal liquefaction, highly dispersed catalysts are especially needed because the catalyst particles are only able to influence reactions within their immediate vicinity.

Laser pyrolysis constitutes a new method for the preparation of ultrafine particle catalysts. This technique is a versatile non-equilibrium thermodynamic process for the production of nanoscale particles involving fast growth and rapid heating/cooling rates (10^3 °/s) which also allows the synthesis of metastable phases. The process involves a gas phase pyrolysis reaction, of two or more molecular species, sustained by the heat generated through the absorption of CO_2 laser energy into vibrational-rotational excitations of at least one of the reactant gas species. Typical reaction temperatures are estimated to be 800-1000°C. A variety of nanoscale particles have been produced using this technique and include MoS_2 , WS_2 , Fe_3C , Fe_2C_3 [1,2].

We have also prepared high surface area (50-86 m^2/g) Mo_2C and Mo_2N ultrafine particles (UFP) by Laser pyrolysis using $\text{Mo}(\text{CO})_6$ as the metal precursor. Previously, Mo_2N and Mo_2C (100-200 m^2/g) have been produced by Temperature Programmed Reduction. This method consists in the reduction of MoO_3 by NH_3 [3,4] or a mixture of H_2/N_2 [5] or CH_4/H_2 [3] for Mo_2N and Mo_2C , respectively. It has been reported that these materials exhibit high activity for heteroatom removal in the hydrotreatment of naphtha and upgrading of coal liquids [6].

Mo_2C and Mo_2N are interstitial alloys formed by the incorporation of carbon, nitrogen and oxygen into the lattice of Mo metal. In these materials, the non-metallic elements (C, N, O) enter into the interstitial sites between metal atoms. Since the bonding among those light elements is very similar, carbonitrides, oxynitrides and oxycarbide phases are possible, depending on the conditions of synthesis [7].

The ability of these materials to incorporate oxygen into their structure is particularly important with respect to their catalytic properties since it has been demonstrated that oxygen together with carbon deposits seriously decrease and/or modify their activity. Therefore it is important to address the nature of the surface of these catalysts as well as to be able to prepare these materials in an oxygen free (or controlled oxygen content) and amorphous carbon free form. For this reason, the role of the precursor and the conditions of preparation are very important.

Several reports have been presented in the literature regarding the effect of chemisorbed oxygen, surface oxide or even intercalated oxygen on the catalytic properties of these materials [8-11]. In these studies, it has been suggested that a certain amount of oxygen in the catalyst may confer a double functionality: that of a Lewis acid as well as of a noble metal [8,10].

This work contains the results from the structural and chemical characterization of Mo_2N and Mo_2C UFP catalysts by X-ray diffraction (XRD), scanning tunneling microscopy (STM), x-ray photoelectron spectroscopy (XPS) and thermogravimetry-mass spectrometry (TG-MS). The main objectives are to elucidate the real composition and surface state of these nanoparticles, to correlate structure and composition with catalytic properties and to determine methods to synthesize them in an oxygen-free and carbon-free form.

EXPERIMENTAL

Details from the experimental apparatus and procedure have been reported elsewhere [1]. Briefly, nanoscale Mo_2N and Mo_2C were synthesized from the reaction of $\text{Mo}(\text{CO})_6$ in the presence of ammonia or ethylene. The catalysts were passivated in a flow of 5% O_2/He for several hours before removal from the reaction chamber.

Mo_2C was also synthesized utilizing MoCl_5 as the metal precursor with the same synthesis parameters that were used for the carbonyl precursor. Table 1 summarizes the reaction conditions employed to synthesize these phases. Notice that the yield of Mo_2C synthesized from MoCl_5 is lower than when $\text{Mo}(\text{CO})_6$ is used.

Synthesis Parameters	Mo ₂ C	Mo ₂ N	Mo ₂ C
Laser Intensity	95W	95W	95W
Chamber Pressure (Torr)	200	200	200
Metal Precursor	Mo(CO) ₆	Mo(CO) ₆	MoCl ₅
Reactant Gas	C ₂ H ₄	NH ₃	C ₂ H ₄
Flow rate (sccm)	80	118	80
Temperature (sublimation cell)	105°C	105°C	150°C
Yield (g product/g precursor)	1.5g/5g	1.5g/5g	50 mg/2 g

CHARACTERIZATION

X-Ray Diffraction

X ray diffraction was used to identify the crystalline phase of the particles as well as to extract average values of the lattice spacing and of the crystallite size of the nanoscale particles. X-ray data were collected using Cu (K α) radiation using a Philips 3100 powder diffractometer. The average particle diameter was estimated from the Debye-Scherrer (DS) equation $D=0.9\lambda/Acos(\Theta_{111})$ [12]. Figure 1 presents the X-ray diffraction data obtained from a Mo₂C UFP. The phase of this carbide has been identified as fcc Mo₂C. The crystallite size calculated for this materials is 2.1 nm which is in good agreement with the value obtained using HRTEM [12].

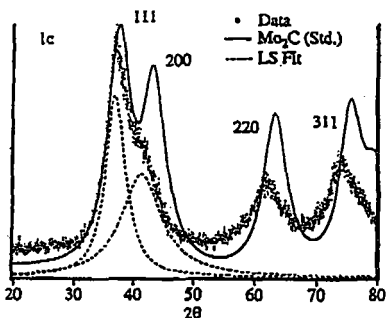


Figure 1
X ray diffractogram of Mo₂C

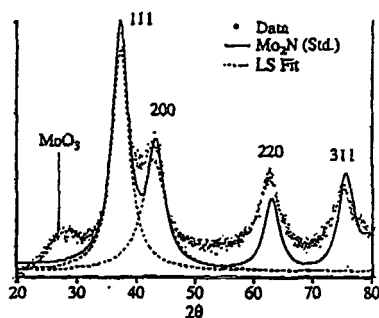


Figure 2
X-Ray diffractogram of Mo₂N

The solid lines in figure 1 correspond to the data generated using a Lorentzian lineshape for the diffraction peaks and an exponential term for the background. The values used for the diffraction peak positions and peak areas were taken from a standard powder diffraction file. The difference in intensities between the standard powder diffraction and the data may be attributed to Mo vacancies in the crystalline structures of the particles or to variations in the metal atom sublattice near the surface. Clear shifts of the diffraction lines toward lower 2θ angles is seen for Mo₂C. This indicates a lattice expansion, presumably associated with the small crystallite size. Figure 2 presents the X-ray diffraction data for Mo₂N which has been identified as fcc Mo₂N. These particles showed an average crystallite size of 2.5 nm.

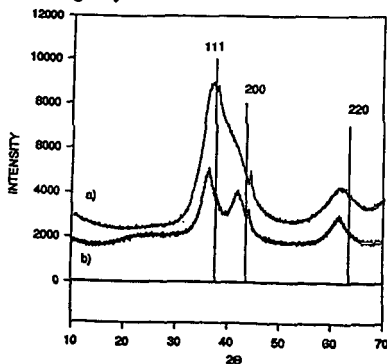


Figure 3
X-ray diffractograms from a) Mo₂C synthesized from Mo(CO)₆ and b) Mo₂C synthesized from MoCl₅.

Figure 3 shows the x-ray diffraction data of Mo_2C synthesized using MoCl_5 . The particle size calculated using the DS equation is 2.4 nm. Notice that now the peaks around $2\theta = 37.7^\circ$ are well resolved and that no sign of MoCl_5 is present. The broad shoulder at $2\theta \sim 25^\circ$ is attributed to the presence of a layer of MoO_3 [2]. High resolution TEM does not show any sign of oxide or carbide coatings. In particular the Mo_2C particles do not appear to have a carbon coating on the surface.

STM

The morphology of atomically flat Au(111) surfaces coated with mono- and multi-layer nanoscale Mo_2N particles was studied using a vacuum STM ($P < 10^{-8}$ torr). The gold substrates were prepared by melting gold wires (0.5 mm diameter) in an acetylene/oxygen flame. These substrates exhibited large atomically flat areas with dimensions of about $100 \times 100 \text{ \AA}^2$ and terraces with single atomic step of approximately 2.4 \AA . The particles were first dispersed in pentane or water solvent. Then they were sonicated for several hours and spin-coated onto the gold substrates. Heat treatment to remove adsorbed water and surface oxide was done in a sample-preparation chamber with a 100 torr of 10% H_2/He mixture. The STM image taken with a Pt/Ir tip is shown in figure 4.

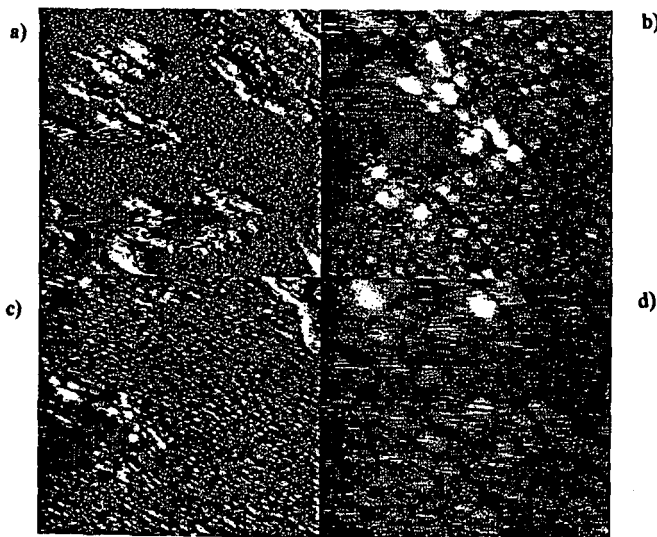


Figure 4

STM images of a layer of Mo_2N UFP deposited on the surface of Au (111) at different magnifications. Each frame corresponds to an area of a) $8000 \times 8000 \text{ \AA}^2$ b) $2000 \times 2000 \text{ \AA}^2$ c) $4000 \times 4000 \text{ \AA}^2$ d) $1000 \times 10000 \text{ \AA}^2$.

It is observed that a monolayer of nanoparticles has been deposited. The underlying terraces of Au(111) can still be observed (Figure 4a). The average particle size deduced from these images is ~ 7 nm. This value is higher than the one observed by TEM, probably because these particles correspond to a different batch from the one used to measure the TEM.

X-Ray Photoelectron Spectroscopy (XPS)

The XPS measurements were performed on a Leybold-Heraeus EA-11 spectrometer using Mg K- α (1253.6 eV) radiation at 15 kV and 20 mA. The oxygen/helium-passivated samples were prepared by pressing the powder into 13 mm diameter pellets. Figure 5 shows the XPS spectra from samples of Mo_2C and Mo_2N that were passivated in oxygen prior to their removal from the laser pyrolysis chamber. Figure 5a corresponds to the photoelectron lines of molybdenum $3d_{5/2}$ and $3d_{3/2}$ from Mo_2N , and figure 5b to the carbon 1s line from the same sample. Figures 5c and 5d correspond to the molybdenum and carbon peaks, respectively, from Mo_2C . The peaks at 228.58 eV in figures 5a and 5c have been assigned to the C-Mo and N-Mo bonding energies, whereas the ones at 232.2 eV to the +VI oxidation state of molybdenum, consistent with the presence of MoO_3 [13,14]. Deconvolution of the data gives 90% of surface molybdenum in the form of oxides (mainly MoO_3) for both Mo_2N and Mo_2C .

The carbon 1s peak in figure 5b, located at 284.5 eV is from carbon presumably formed

during synthesis. No evidence was found of the presence of a carbidic surface phase in the molybdenum nitride sample. Deconvolution of the carbon photoelectron line from the molybdenum carbide sample gives two peaks at 283.7 eV and 284.5 eV which correspond to a mixture of carbidic carbon and amorphous carbon [13].

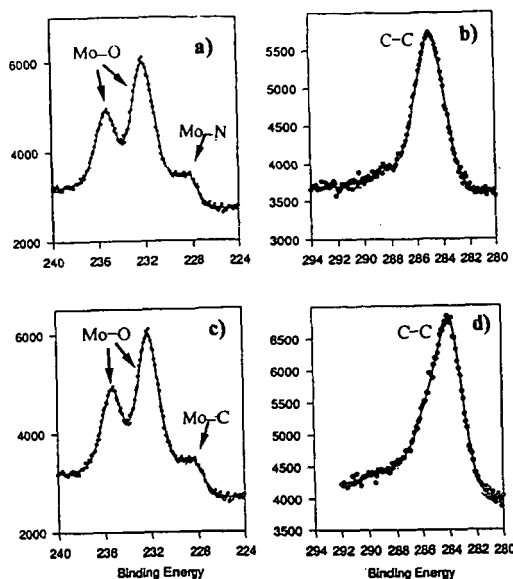


Figure 5
XPS data of Mo_2N and Mo_2C synthesized from the decomposition of $\text{Mo}(\text{CO})_6$

Thermogravimetry-Mass Spectrometry (TG-MS)

Mo_2C and Mo_2N synthesized from the decomposition of $\text{Mo}(\text{CO})_6$ were also studied with TG-MS. This technique provided valuable information about the surface composition and the extent of oxygen present on the catalyst. Between 5 and 7 mg of fresh catalyst (Mo_2N or Mo_2C) were loaded on the TG system and were flushed with He at room temperature for about 30 minutes. Pure He, and He mixed with 50% hydrogen were used as carrier gases in these experiments. The temperature program consisted on heating the samples from room temperature to 100°C. The samples were maintained at this temperature for 5 minutes, then they were heated to 900°C at a constant rate of 1°C/s. During the temperature ramp, the composition of the gas leaving the TG was monitored using a mass spectrometer.

Figure 6 shows the TG trace together with the mass signal from Mo_2C reduced in hydrogen. It is observed that there are three regions of weight loss in this sample. The first region at about 2 minutes (100°C) corresponds to the desorption of adsorbed water on the material. In the second temperature region from 8 to 12 minutes (200-410°C), oxygen is being removed from the sample in the form of water. The desorption of water occurs in the form of a broad peak that starts at about 200°C and which has a maximum at 540°C. There is still some water desorbing simultaneously with CO at a temperature about 620°C. The presence of CO indicates that some oxygen from the sample is reacting with carbon from the material. At about 540°C carbon is being removed from the sample in the form of CH_4 with a maximum removal at 740°C.

Notice also that after 18 minutes (800°C), water continues to desorb indicating that even at this temperature oxygen has not been completely removed from the samples. Oxygen desorbed in the form of water below 500°C has been assigned to surface oxygen and near-surface oxygen [15] whereas that desorbed above that temperature has been assigned to the removal of deeper lying oxygen that has diffused from the particle interior to the surface.

In figure 7 the TG trace from Mo_2N is presented. This catalyst experienced a total weight loss of about 25%. Most of it comes from oxygen removal in the form of water. The water evolved at temperatures below 340°C has been assigned to surface oxygen and near-surface oxygen whereas water evolved above this temperature has been assigned to bulk oxygen. Although no ammonia was detected in the gases evolved, it is observed that at about 800°C the nitride decomposes by losing molecular nitrogen. Since no methane evolved from the heat treatment of Mo_2N , it follows that the methane detected from the carbide corresponds to carbidic carbon that has reacted with hydrogen, and that amorphous carbon was not removed

from the sample. This agrees with reports that this carbon is very difficult to remove [15].

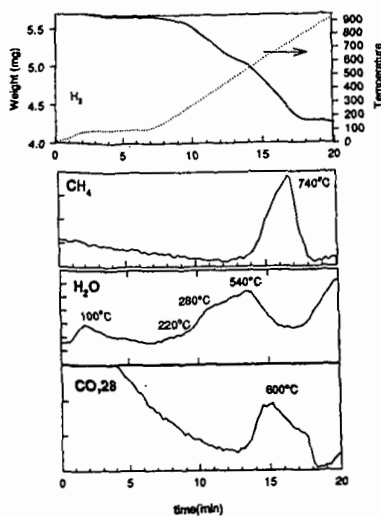


Figure 6
TG-MS trace of Mo_2C treated in hydrogen

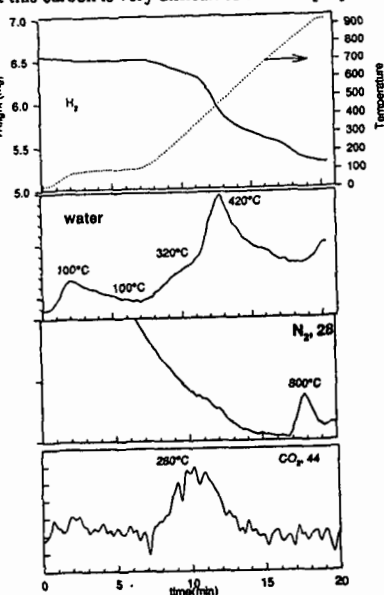


Figure 7
TG-MS trace of Mo_2N treated in hydrogen.

CONCLUSIONS

Fcc Mo_2N and Mo_2C have been synthesized from the decomposition of $\text{Mo}(\text{CO})_6$ and MoCl_5 using Laser Pyrolysis. From the structural point of view, they appear crystalline with little or no disorder. Even though HR-TEM did not show any sign of oxide or carbide coating on the particle, XPS indicated that a large percentage of Mo atoms on the surface are in the form of an oxide phase produced during surface passivation. In addition, carbon was observed to be present on the surface of both catalysts from the decomposition of the metalorganic precursor. TG-MS shows that oxygen content constitutes a major contaminant on these particles and that polymeric carbon is very difficult to remove.

REFERENCES

- [1] X.X. Bi, B. Ganguly, G.P. Huffman, F.E. Huggins, M. Endo, P.C. Eklund, *J. Mater. Res.* 8(7), (1993) 1666.
- [2] X.X. Bi, Y. Wang, W.T. Lee, K.A. Wang, S. Bandow and P.C. Eklund, *Mat. Res. Soc. Symp. Proc.*, 327, (1994) 47-52.
- [3] S.T. Oyama, J.C. Schlatter, J. Metcalfe, J. Lambert, *Ind. Eng. Chem. Res.* 27, (1988) 1648-1653.
- [4] J.-G. Choi, R. L. Curl, L.T. Thompson, *J. of Catal.* 146, (1994) 218-227.
- [5] R.S. Wise, E.J. Markel, *J. of Catal.* 145, (1994) 344-355.
- [6] S.T. Oyama, R. Kapoor, C. Shudakar, *Prep. of Am. Chem. Soc. Div. Fuel Chemistry*, 37(1), (1992) 233.
- [7] S.T. Oyama, *Catalysis Today*, 15 (1992) 179-200
- [8] H.S. Kim, G. Bugli, G. Djega-Mariadassou, *Proc. Mater. Res. Soc. Symposium T*, Nov 29-Dec. 1 1994.
- [9] M. Ledoux, *Proc. Mater. Res. Soc. Symposium T*, Nov. 29-Dec 1 1994.
- [10] F. H. Ribeiro, R.A. Dalla Betta, M. Boudart, J. Baumgartner, E. Iglesia, *J. of Catal.* 130, (1991)86-105.
- [11] G.S. Ranhotra, A.T. Bell, J.A. Reimer, *J. of Catal.* 108, (1987) 40-49.
- [12] X.X. Bi, K.D. Chowdhury, R. Ochoa, W.T. Lee, S. Bandow, M.S. Dresselhaus, P.C. Eklund in *Proc. of Materials Res. Society Symposium T*, Fall 1994, in press.
- [13] M. J. Ledoux, C.P. Huu, J. Guille, H. Dunlop, *J. of Catal.*, 134, (1992) 383.
- [14] C.D. Wagner, W.M. Riggs, L.E. Davis, J.F. Moulder, and G.E. Muilenberg in "Handbook of X-ray Photoelectron Spectroscopy". Perkin-Elmer, Eden Prairie, MN, 1979.
- [15] K.J. Leary, J. N. Michaels, A.M. Stacy, *J. of Catalysis* 101, (1986)301-313.